Correlations and Synchrony in Threshold Neuron Models

Tatjana Tchumatchenko,[1,2] Aleksey Malyshev,[3,4] Theo Geisel,[1] Maxim Volgushev,[3,4,5] and Fred Wolf[1]

[1]*Max Planck Institute for Dynamics and Self-Organization and Bernstein Center for Computational Neuroscience, Göttingen, Germany*

[2]*Göttingen Graduate School for Neurosciences and Molecular Biosciences, Göttingen, Germany*

[3]*Inst. of Higher Nervous Activity and Neurophysiology, RAS, Moscow, Russia*

[4]*Department of Psychology, University of Connecticut, Storrs, Connecticut, USA*

[5]*Department of Neurophysiology, Ruhr-University, Bochum, Germany*

(Received 20 October 2008; revised manuscript received 29 May 2009; published 4 February 2010)

We study how threshold models and neocortical neurons transfer temporal and interneuronal input correlations to correlations of spikes. In both, we find that the low common input regime is governed by firing rate dependent spike correlations which are sensitive to the detailed structure of input correlation functions. In the high common input regime, the spike correlations are largely insensitive to the firing rate and exhibit a universal peak shape. We further show that pairs with different firing rates driven by common inputs in general exhibit asymmetric spike correlations.

DOI: 10.1103/PhysRevLett.104.058102 PACS numbers: 87.19.lm, 05.40.−a, 87.19.ll, 87.19.lt

Correlated neural activity can reflect specific features of sensory stimuli or behavioral tasks [1]. Recently, the origin, statistical structure and coding properties of spike correlations have attracted substantial attention [2–6]. How do neurons transfer correlated inputs into correlated output? In the past, this fundamental question was often addressed using the Fokker Planck formalism [5,7]. However, these approaches are technically very demanding and allowed for explicit expressions in special limits only.

Here we show that an alternative modeling framework, based on the threshold crossings of smooth random functions [8,9], can provide a mathematically transparent and highly tractable description of spike correlations driven by inputs of arbitrary temporal structure and correlation strength. Our theoretical findings may also find applications beyond neuroscience, e.g., in spin ordering reliability studies, as the statistics of (upward) level crossings is a general, long standing problem in physics and engineering [9]. We calculate quantities which have so far escaped a theoretical description by the competing Fokker-Planck based formalism: (1) peak spike correlation for arbitrary input correlation strength, (2) rate independent peak shape in the high correlation regime, (3) complete spike correlation function for weak correlations, and (4) asymmetric spike correlation function in pairs with different rates [10]. *A priori*, the simple threshold model used cannot be expected to completely capture the complex behavior of cortical neurons. Nevertheless, our experiments strongly suggest that it is capable of describing spike correlations in cortical neurons with good accuracy. In particular, our experiments reproduce and extend previous reports on the firing rate dependence of cortical spike correlations [4,5] and qualitatively confirm all new predictions derived here.

Model framework.—Each neuron in a network receives inputs from thousands of presynaptic neurons. This bombardment generates a fluctuating net synaptic current and a fluctuating voltage at the soma. These fluctuations are frequently modeled by an effective Gaussian input current with temporal correlations shaped by the synaptic responses [10,11]. The simplest conceivable model of spike generation from a fluctuating voltage $V(t)$ identifies the spike times t_j with upward crossings of a threshold voltage ψ_0. The times t_j determine the spike train:

$$s(t) = \sum_j \delta(t - t_j) = \delta(V(t) - \psi_0)|\dot{V}(t)|\theta(\dot{V}(t)), \quad (1)$$

$\delta(\cdot)$ and $\theta(\cdot)$ are the Dirac delta and Heaviside theta functions, respectively. We assume a differentiable $C(\tau) = \langle V(t)V(t+\tau)\rangle$, see [9,10]. This model has no reset but exhibits an intrinsic silence period after a spike. We quantify the decay of $C(\tau)$ near zero using the differential correlation time $\tau_s = \sqrt{C(0)/|C''(0)|}$. We derive somatic voltage $V(t)$ assuming a simple leaky integrator with a membrane time constant τ_M, $\tau_M\dot{V}(t) = -V(t) + \xi(t)$. $C(\tau)$ can then be derived from the current correlation function $C_I(\tau) = \langle\xi(t)\xi(t+\tau)\rangle$:

$$\tilde{C}(\omega) = \tilde{C}_I(\omega)/(1 + \tau_M^2\omega^2), \quad (2)$$

where $\tilde{C}_I(\omega)$ and $\tilde{C}(\omega)$ are the Fourier transforms of $C_I(\tau)$ and $C(\tau)$, respectively. For concreteness, we choose an exponentially decaying correlation function consistent with experimental observations [11]

$$c(\tau) = 1/\cosh(\tau/\tau_s), \quad \langle V(t)V(t+\tau)\rangle = \sigma_V^2 c(\tau). \quad (3)$$

In a network, any two neurons can have common presynaptic partners which lead to a common synaptic component n_C, Fig. 1(a)[10]. To model this situation, we consider a shared synaptic component n_C and the individual components n_j, as in Fig. 1(a). The net synaptic current $\xi_j(t)$ of neuron j is given by

$$\xi_j(t) = \sqrt{1 - r_{\text{in}}}\, n_j(t) + \sqrt{r_{\text{in}}}\, n_c(t), \tag{4}$$

where r_{in}, $0 \le r_{\text{in}} < 1$, is the input correlation strength. We model all three n_C, n_1, n_2 as statistically independent Gaussian processes with the same temporal correlation $C_I(\tau)$ and zero mean. Because in a Gaussian ensemble any expectation value is completely determined by pairwise covariances, all pairwise $\langle s_i(t) s_j(t+\tau)\rangle$ can be obtained from the joint Gaussian probability density of $\vec{k} = (V_1(0), \dot{V}_1(0), V_2(\tau), \dot{V}_2(\tau))$ $p(\vec{k}) = \exp(-\vec{k}^T C^{-1} \vec{k}/2)/(4\pi^2\sqrt{\text{Det}C})$ where

$$C = \begin{pmatrix} \sigma^2_{V_1} & 0 & C_{12}(\tau) & C'_{12}(\tau) \\ 0 & \sigma^2_{\dot{V}_1} & -C'_{12}(\tau) & -C''_{12}(\tau) \\ C_{12}(\tau) & -C'_{12}(\tau) & \sigma^2_{V_2} & 0 \\ C'_{12}(\tau) & -C''_{12}(\tau) & 0 & \sigma^2_{\dot{V}_2} \end{pmatrix}. \tag{5}$$

Matrix entries are $C_{ij} = \langle k_i k_j \rangle$. The voltage cross correlation function $C_{12}(\tau)$ is:

$$C_{12}(\tau) = \langle V_1(0) V_2(\tau)\rangle = r \sigma_{V_1} \sigma_{V_2} c(\tau). \tag{6}$$

Here $C'_{12}(\tau)$ and $C''_{12}(\tau)$ are derivatives of $C_{12}(\tau)$. Note that with additional noise sources voltage correlation r can be smaller than the correlation of injected currents, $r \le r_{\text{in}}$ [10,12]. The firing rate $\langle s(t)\rangle$ of a neuron is:

$$\nu = \langle s(t)\rangle = \exp[-\psi_0^2/(2\sigma_V^2)]/(2\pi\tau_s). \tag{7}$$

The firing rate in Eq. (7) depends only on two parameters: the correlation time and the threshold-to-variance ratio ψ_0^2/σ_V^2, but not on the specific choice of the correlation function [9]. Hence, processes with the same τ_s but different form of $C(\tau)$ will have the same ν, despite different temporal spike statistics. The ratio ψ_0/σ_V determines the probability of threshold crossings, a decrease in ψ_0/σ_V leads to an increase in ν. Injections of constant currents shift the mean potential and thus decrease the distance to threshold ψ_0, resulting in a higher ν. ν is also increasing with decreasing τ_s, because faster fluctuations lead to a higher rate of threshold crossings. This model has a maximal firing rate $\tilde{\nu} = 1/(2\pi\tau_s)$, and should therefore be used

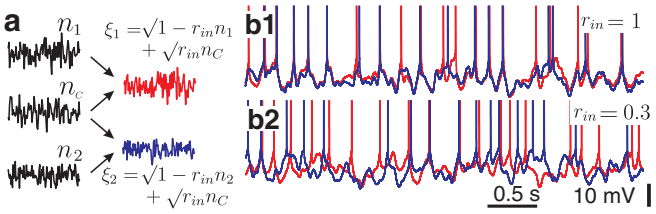

FIG. 1 (color online). (a) The generation two fluctuating currents ξ_1, ξ_2 with a correlation strength r_{in}. ξ_1 and ξ_2 are injected successively into neurons [4,5] to mimic neuronal cross correlations *in vivo*. (b) Voltage traces of two neurons (red [medium gray] and blue [dark gray]) subject to currents with $r_{\text{in}} = 1$ (b1) and $r_{\text{in}} = 0.3$ (b2). In all four recordings $\nu \approx 5$ Hz, $\tau_s = 20$ ms and $C_I(\tau)$ as in Eqs. (2) and (3).

in the fluctuation driven, low firing rate $\nu < \tilde{\nu}$ regime important for cortical neurons [6].

Experimental test.—Correlated fluctuating currents resembling net synaptic currents at the soma *in vivo* [11] were injected somatically into layer 2/3 pyramidal neurons *in vitro* ($N = 19$) in neocortical slices from rats (PND 22–27). To emulate temporal correlations *in vivo* [11], we chose the current correlation $C_I(\tau) = \mathcal{F}^{-1}[\tilde{C}(\omega) \times (1 + \tau_M^2 \omega^2)]$ where $\tilde{C}(\omega) = \mathcal{F}(C(\tau))$ and $C(\tau)$ as in Eq. (3), $\mathcal{F}$ denotes the Fourier transform. We assumed $\tau_M = 20$ ms for all cells. We fixed the input correlation strength across trials $r_{\text{in}} = 0.3$, 1 and set $\tau_s = 20$, 100 ms. The varying input cross correlation r_{in} across trials mimics the fraction r_{in} of common presynaptic partners in this frequently used experimental paradigm [4,5]. In the recordings (10 s or 5 s episodes), we targeted two different firing rates $\nu_1 = 5$ Hz ($T_1 = 10$ s), $\nu_2 = 10$ Hz ($T_2 = 5$ s), by injection of an additional constant current. The average firing rate ν_m is the average number of spikes in a recording divided by T and averaged over trials and cells. We obtained a total of $N = 281$ recordings for ν_1, $N = 299$ recordings for ν_2. For identical noise injection ($r_{\text{in}} = 1$) we recorded $N = 80$ at the target rate ν_1, $N = 81$ at ν_2, and $N = 21$ at a target rate of 3 Hz ($T_3 = T_1$). Figure 1(b) shows examples of recorded voltage traces for large and small r_{in}. We estimated $\nu_{\text{cond}}(\tau)$ by pooling trials from the same and different cells ($\ge$4 cells, for any parameter set), cross correlating all trials for a given parameter set $\{r, \tau_s, \nu\}$ and using a Gaussian filter kernel with $\sigma = 5$ ms and 95% Jackknife confidence intervals for N random subsamples each containing $N/2$ recordings.

Spike correlations.—To quantify the temporal spike cross correlations between neuron 1 and 2 we used the conditional firing rate $\nu_{\text{cond}}(\tau)$:

$$\nu_{\text{cond}}(\tau) = (\nu_1 \nu_2)^{-1/2} \langle s_1(t) s_2(t+\tau)\rangle. \tag{8}$$

For $\nu_1 = \nu_2$, $\nu_{\text{cond}}(\tau)$ is the firing rate of neuron 2 triggered on the spikes of neuron 1. $\nu_{\text{cond}}(\tau)$ measures correlations on all time scales and is equivalent to the correlation coefficient ρ ($\rho \approx T[\nu_{\text{cond}}(0) - \nu]$) for small time bin T [5]. In a neuronal pair with $\nu_1 = \nu_2$, $\nu_{\text{cond}}(\tau)$ is a symmetrical function which approaches ν as τ increases and maximally deviates from ν at $\tau = 0$. We obtained $\nu_{\text{cond}}(0)$ by solving the Gaussian integrals in Eqs. (5) and (8) [10]:

$$\nu_{\text{cond}}(0) = \tilde{\nu}\left(\frac{\nu}{\tilde{\nu}}\right)^R [1 + 2r \arctan(\sqrt{R^{-1}})/\sqrt{1 - r^2}], \tag{9}$$

where $R = (1 - r)/(1 + r)$. Equation (9) predicts a nonlinear increase of $\nu_{\text{cond}}(0)$ with r, see Fig. 2(a).

Spike correlations for $r \approx 1$.—Here, the correlation peak is independent of ν and the functional form of $C_{12}(\tau)$:

$$\nu_{\text{cond}}(0) \approx 1/(2\sqrt{2}\sqrt{1 - r}\tau_s) \qquad (r \approx 1). \tag{10}$$

Does this prediction hold for neuronal spike correlations? Figure 3 (left) depicts recorded $\nu_{\text{cond}}(\tau)$ in the high r regime for different firing rates. The correlation peaks for

3, 5.3 and 8.5 Hz are very similar [Fig. 3 (left)]. These recordings indicate that the peak magnitude can be largely insensitive to the firing rate. In fact the entire peak shape appears firing rate independent. To assess this phenomenon further, we calculate $\nu_{\mathrm{cond}}(\tau)$ by solving the Gaussian integrals in Eqs. (1) and (5), for $r \approx 1$ and $\tau \ll \tau_s$ [10]:

$$\nu_{\mathrm{cond}}(\tau) = 1/(4\tau_s^*)(2 - 3\hat{\tau}^2 + 30/8\hat{\tau}^4) + O(\tau^6), \quad (11)$$

where $\hat{\tau} = \tau/\tau_s^*$ with the time constant $\tau_s^* = \sqrt{2}\sqrt{1-r}\tau_s$. Equation (11) is insensitive to the functional form of $C_{12}(\tau)$ [Fig. 2(b)] and bears resemblance to the limit definitions of the δ peak, which is present at the origin of the auto conditional firing rate [10]. Equation (11) thus further supports the existence of a rate independent universal peak shape and height. Notably, we find a good qualitative agreement between the experiment and simulated $\nu_{\mathrm{cond}}(\tau)$ (Fig. 3). The recorded salient correlation peak structure bears the signatures of the emerging correlation peak as described by Eq. (11) and the width and height of the common peak can be qualitatively described by the theoretical curves in Fig. 3 (right). A moderate firing rate dependence is reasonable for $\tau = 0$ because the effective voltage correlation $r = 0.72 < r_{\mathrm{in}}$ is reduced due to additional noise sources [10,12]. In addition to fluctuation driven firing considered in our framework, the measured $\nu_{\mathrm{cond}}(\tau)$ (Figs. 3 and 4) exhibit weak periodic modulations of the stationary tails which are not included in our framework. These additional weak modulations are more prominent at higher firing rates and might result from depolarization dependent subthreshold oscillations [13] or the contribution of mean-driven firing [14].

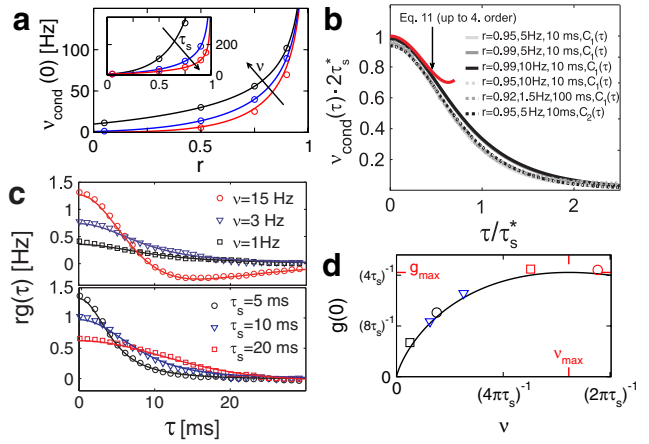

FIG. 2 (color online). Pairwise spike correlations. (a) $\nu_{\mathrm{cond}}(0)$ vs r as in Eq. (9); $\nu_{\mathrm{cond}}(0)$ for $\tau_s = 10$ ms and $\nu = 0.1$ Hz (red [medium gray]), $\nu = 1$ Hz (blue [dark gray]), $\nu = 10$ Hz (black). [(a), inset] $\nu_{\mathrm{cond}}(0)$ for $\nu = 5$ Hz and $\tau_s = 10$ ms (red [medium gray]), $\tau_s = 5$ ms (blue [dark gray]), $\tau_s = 1$ ms (black); circles denote simulated results. (b) $2\tau_s^*\nu_{\mathrm{cond}}(\tau)$ vs τ/τ_s^* for simulations and Eq. (11) (red [medium gray]); $C_1(\tau)$ as in Eq. (3), $C_2(\tau) = \frac{\sigma_V^2 \cos(\tau/(\sqrt{2}\tau_s))}{\cosh(\tau/(\sqrt{2}\tau_s))}$. (c) $rg(\tau)$ vs τ as in Eq. (12) and simulated results for $r = 0.05$ (top) $\nu = 15$, 3, 1 Hz, $\tau_s = 10$ ms. (bottom) $\tau_s = 5$, 10, 20 ms, $\nu = 5$ Hz. (d) $g(0)$ vs ν as in Eq. (13), $\nu_{\max}$ and $g_{\max}$ (red [medium gray] bars), symbols show $g(0)$ from (c).

Weak correlations.—We obtain $\nu_{\mathrm{cond}}(\tau) = \nu + rg(\tau) + O(r^2)$ by solving the Gaussian integrals in Eqs. (1), (5), and (8) assuming $rc(\tau) \ll 1$ [10]. In linear order, spike correlations depend on ν and $c(\tau)$:

$$g(\tau) = \nu[c(\tau)|2\log(\nu/\tilde{\nu})| - \pi/2\tau_s^2 c''(\tau)] \quad (12)$$

$$g(0) = \nu[|2\log(\nu/\tilde{\nu})| + \pi/2]. \quad (13)$$

Figure 2(c) illustrates the dependence of $g(\tau)$ on τ_s and ν. Equation (12) implies that spike correlations are typically narrower than the underlying voltage correlations, due to the admixture of $c''(\tau)$ which has a shorter time scale than $c(\tau)$ [10]. Notably, this is consistent with previous reports (p. 367 in [3]). Equation (13) implies that the correlation peak ($\nu_{\mathrm{cond}}(0) - \nu$) is increasing with ν [Figs. 2(c) and 2(d)], in agreement with [5]. However, the percentage of simultaneous spikes ($[\nu_{\mathrm{cond}}(0) - \nu]/\nu$) is higher for lower rates, as previously reported [Figs. 3(B,C) in [4]]. These seemingly contradictory findings are explained by the nonlinear form of $g(0) \propto \nu|\log(\nu/\tilde{\nu})|$. $g(0)$ is maximal $g_{\max} = 2\nu_{\max}$ for the rate $\nu_{\max} = \exp(\pi/4 - 1)/(2\pi\tau_s)$ [Fig. 2(d)]. This simple model qualitatively captures the correlation peak for weakly correlated, low firing rate neurons (Fig. 4). The ν dependence predicted by Eq. (13) is reflected in Figs. 4(b) and 4(c), even though $\nu_m = 9.4$ Hz escapes direct comparison ($\nu_m > \tilde{\nu}$).

Rate differences.—The correlation matrix in Eq. (5) includes $c'(\tau)$, which so far did not enter $\nu_{\mathrm{cond}}(\tau)$. As $c'(\tau)$ is an antisymmetric function it is conceivable that a rate difference ($\nu_1 \neq \nu_2$) will lead to asymmetric $\nu_{\mathrm{cond}}(\tau)$. In the linear r regime, we obtain $g(\tau) = [\nu_{\mathrm{cond}}(\tau) - \sqrt{\nu_1\nu_2}]/r$ via Eqs. (1), (5), and (8) [10]:

$$g(\tau) = \sqrt{\nu_1\nu_2}[c(\tau)e_1e_2 - \pi/2\tau_s^2 c''(\tau) - c'(\tau)\tau_s\Delta], \quad (14)$$

where $e_i = \psi_0/\sigma_{V_i}$ and $\Delta = \sqrt{\pi/2}(e_2 - e_1)$. The peak position is no longer at $\tau = 0$ but is shifted to $\tau_{\mathrm{Peak}} = \tau_s\Delta/[e_1e_2 + \pi c^{(4)}(0)\tau_s^4/2]$. The spikes of the higher rate

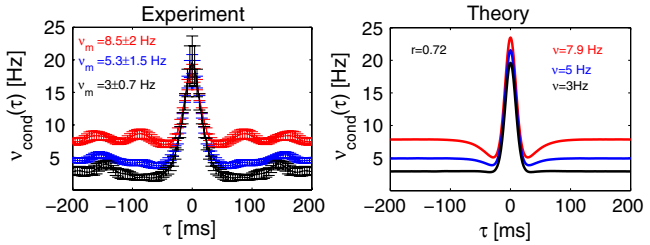

FIG. 3 (color online). Firing rate independence of spike correlations for strong input correlations, theory and experiment. (left) $\nu_{\mathrm{cond}}(\tau)$ vs τ for $r_{\mathrm{in}} = 1$. (right) $\nu_{\mathrm{cond}}(\tau)$ in a simulated pair with $\nu_1 = 3$ Hz (black), $\nu_2 = 5$ Hz (blue [dark gray]), $\nu_3 = 7.9$ Hz (red [medium gray]) with $\tau_s = 20$ ms and $r = 0.72$, consistent with effective voltage correlation strength [10].

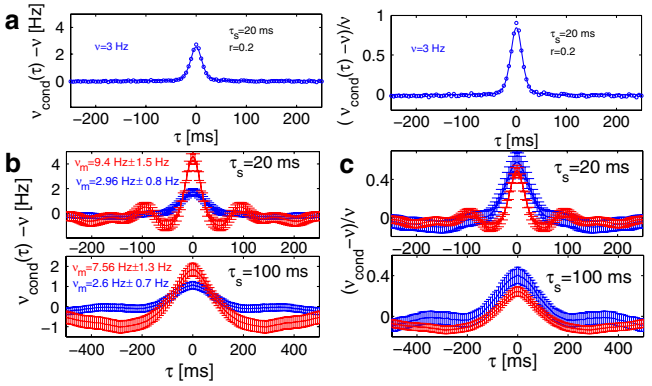

FIG. 4 (color online). Firing rate dependence of weak spike correlations, theory and experiment. (a) $\nu_{\mathrm{cond}}(\tau) - \nu$ vs τ and $[\nu_{\mathrm{cond}}(\tau) - \nu]/\nu$ vs τ for $\nu = 3$ Hz, $\tau_s = 20$ ms and $r = 0.2$, which is consistent with effective voltage correlation strength [10]; circles denote simulated results. (b),(c) measured $\nu_{\mathrm{cond}}(\tau) - \nu$ vs τ and $[\nu_{\mathrm{cond}}(\tau) - \nu]/\nu$ vs τ for $\tau_s = 20$, 100 ms.

neuron precede the spikes of the lower rate neuron. This asymmetry increases with increasing Δ and increasing τ_s. The predicted asymmetric $\nu_{\mathrm{cond}}(\tau)$ [Fig. 5 (left)] is in good agreement with experimental results [Fig. 5 (right)]. The measured peak shift increases with τ_s. This τ_s dependence is in qualitative agreement with Eq. (14), even though experiments with $\tau_s = 100$ ms escape direct quantitative comparison as $\nu_m > \tilde{\nu} \approx 1.6$ Hz. Notably, shifted correlations are well known in the biological literature and are often interpreted as indications of synaptic connections or input delays [15]. Our model reveals a potential mechanism for the occurrence of asymmetric correlations in pairs with synchronous inputs [3].

Discussion.—We presented a framework for the description of cross correlations of upward level crossings with arbitrary functional form of input correlations. Our results confirm previous reports on the rate dependence of spike correlations [4,5]. This behavior, however, holds for weak correlations only. With strongly correlated inputs, spike correlations become independent of the firing rate but

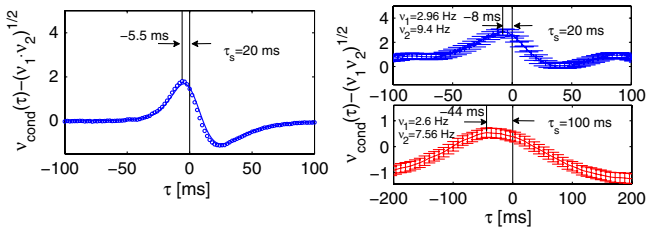

FIG. 5 (color online). Difference in firing rates leads to asymmetric spike correlations. (left) $\nu_{\mathrm{cond}}(\tau) - \sqrt{\nu_1 \nu_2}$ vs τ, simulated results and Eq. (14) for $r = 0.2$, $\nu_1 = 2.65$ Hz, $\nu_2 = 3\nu_1$ and $\tau_s = 20$ ms. Arrows denote the peak position. (right) experimentally measured $\nu_{\mathrm{cond}}(\tau) - \sqrt{\nu_1 \nu_2}$ vs τ for $\tau_s = 20$, 100 ms.

depend on the correlation time of voltage fluctuations. In cell pairs with rate differences the temporal symmetry of spike correlations is lost. Finally, let us stress that input correlations modeled in our framework do not imply a particular connectivity as they can arise from common input or reciprocal connections. Identifying self-consistent choices of $c(\tau)$, r, $\psi_{0,i}$, $\sigma_{V,i}$ in a network of prescribed connectivity will be a fruitful direction of future research.

We thank E. Nikitin for experimental assistance, A. Witt for help with statistical analysis and the Bundesministerium für Bildung und Forschung (No. 01GQ0430), German-Israeli Foundation (No. I-906-17.1/2006), Federal Program of Russian Department of Education and Russian Foundation for Basic Research for financial support.

[1] C. M. Gray *et al.*, Nature (London) **338**, 334 (1989); E. Zohary *et al.*, Nature (London) **370**, 140 (1994); A. K. Kreiter and W. Singer, J. Neurosci. **16**, 2381 (1996).
[2] M. D. Binder and R. K. Powers, J. Neurophysiol. **86**, 2266 (2001); M. Volgushev *et al.*, J. Neurosci. **26**, 5665 (2006); T. Gollisch and M. Meister, Science **319**, 1108 (2008); J. W. Pillow *et al.*, Nature (London) **454**, 995 (2008); S. Ostojic *et al.*, J. Neurosci. **29**, 10234 (2009).
[3] I. Lampl *et al.*, Neuron **22**, 361 (1999).
[4] G. Svirskis and J. Hounsgaard, Network **14**, 747 (2003);
[5] J. de la Rocha *et al.*, Nature (London) **448**, 802 (2007); E. Shea-Brown *et al.*, Phys. Rev. Lett. **100**, 108102 (2008).
[6] D. S. S. Greenberg *et al.*, Nat. Neurosci. **11**, 749 (2008).
[7] B. Lindner, Phys. Rev. E **69**, 022901 (2004); R. Moreno-Bote and N. Parga, Phys. Rev. Lett. **96**, 028101 (2006).
[8] P. Jung, Phys. Lett. A **207**, 93 (1995); Y. Burak *et al.*, Neural Comput. **21**, 2269 (2009).
[9] M. Kac, Am. J. Math. **65**, 609 (1943); S. O. Rice, Bell Syst. Tech. J. **23**, 282–332 (1944); **24**, 46–156 (1945); B. Derrida, V. Hakim, and R. Zeitak, Phys. Rev. Lett. **77**, 2871 (1996).
[10] See supplementary material at http://link.aps.org/supplemental/10.1103/PhysRevLett.104.058102: Eq. 4 (sec. 1.1), intrinsic noise sources (sec. 1.2), properties of $c(\tau)$ and Eq. 3 (sec. 2.1) Eq. 7 (sec. 2.2), Eq. 9 (sec. 2.6), Eq. 10,11 (sec. 2.5), Eq. 12,13 (sec. 2.3), Eq. 14 (sec. 2.4).
[11] A. Destexhe *et al.*, Nat. Rev. Neurosci. **4**, 739 (2003).
[12] Z. F. Mainen and T. J. Sejnowski, Science **268**, 1503 (1995); E. Schneidman *et al.*, Neural Comput. **10**, 1679 (1998); G. A. Jacobson *et al.*, J. Physiol. **564**, 145 (2005).
[13] Y. Amitai, Neuroscience (Oxford) **63**, 151 (1994); Y. Gutfreund, Y. Yarom, and I. Segev, J. Physiol. **483**, 621 (1995).
[14] N. Brenner *et al.*, Phys. Rev. E **66**, 031907 (2002); W. Gerstner and W. M. Kistler, *Spiking Neuron Models* (Cambridge Univ. Press, Cambridge, 2002).
[15] D. Ts'o *et al.*, J. Neurosci. **6**, 1160–1170 (1986); J. J. Eggermont, *The Correlative Brain: Theory and Experiment in Neural Interaction* (Springer Verlag, Berlin, 1990); S. Fujisawa *et al.*, Nat. Neurosci. **11**, 823–833(2008).